BNL-104682-2014-TECH

AGS/AD/Tech Note No. 264;BNL-104682-2014-IR

BEAM INDUCED RADIOACTIVITY AROUND THE AGS RING

K. A. Brown

September 1986

Collider Accelerator Department

Brookhaven National Laboratory

U.S. Department of Energy

USDOE Office of Science (SC)

DISCLAIMER

Accelerator Division
Alternating Gradient Synchrotron Department
BROOKHAVEN NATIONAL LABORATORY
Associated Universities, Inc.
Upton, New York 11973

Accelerator Division
Technical Note

No. 264

BEAM INDUCED RADIOACTIVITY AROUND THE AGS RING

September 26, 1986

K.A. Brown and M. Tanaka

$ I. Introduction

The AGS beam intensity has been steadily increasing by continuous efforts in improving operational conditions and in updating machine components and instrumentations(e.g. during the 1986 spring FEB run, 1.6 to 1.8 * 10**13 ppp has been continuously accelerated). In addition, the number of available operation modes has also increased, i.e., SEB, FEB (with SBE), Polarized Protons, and Heavy Ions. Beam-loss induced radioactivity is also increasing and exposure to it accounts for a major part of the doses received by the AGS personnel.

It is getting very important to take, more periodically, complete and reproducible data of the residual radiation due to activation around the AGS ring and to try to understand the azimuthal and time structure of its distribution, not only for radiation safety but also for beam diagnostics and extrapolation to higher beam intensity operation.

In this note health physics and machine data will be presented for different machine running conditions. From this data comparisons will be made with the expectation that the dose rates in certain areas can be predicted based on beam losses.

$II. The Relationship Between Dose and Beam Loss

The radiation in the AGS is caused by beam losses at different energies and by the associated cascade particles also caused by the beam losses. Therefore it is given that the dose absorbed is proportional to the number of particles lost at different energies. If we call the dose measured D and the number of particles lost $\mathcal{F}$, then,

$$D \propto \mathcal{F}.$$

It has already been established that for induced activity where many radionuclides have been produced that the rate of decay can be approximated by (see Ref. 1),

$$\ln\left(\frac{T+t}{t}\right),$$

where T is the irradiation time and t is the cooldown time. Therefore the dose rate can be taken as,

$$\dot{D} \propto \mathcal{F} \cdot \ln\left(\frac{T+t}{t}\right).$$

By introducing a proportionality constant k, then,

$$\dot{D} = k \cdot \mathcal{F} \cdot \ln\left(\frac{T+t}{t}\right)$$

If comparisons made by estimating k are found to be consistant then it will be possible to estimate the dose rate based simply on beam losses.

$ III. Health Physics Data

After turning off the beam for a shutdown, a complete residual radiation survey of the AGS ring is conducted by Health Physics (HP) personnel as a safty procedure. The highest radiation levels at one foot from the beam pipe (inside and outside of the ring) in the straight sections between the main magnets (the highest level is typically the downstream end) are measured with XETEX 302 Digital Exposure Ratemeters, which can cover a dose range from 0.01 mR/h to 99.9 R/h with an estimated accuracy of +/- 15%. A complete recorded survey requires three HP personnel and takes approximately 1 and 1/4 hours. The present RLRM radiation monitor system, which consists of 120 5 m long and 2.22 cm diameter ion chambers, mounted on the main magnet girders, is quite useful for normal beam intensity but not for activation measurements nor for low beam intensity opertation (< 10**10 ppp).

Results (outside HP data) of the following recent ring radiation surveys have been plotted in Figures 1, 2, 3, & 4. There are no significant differences between the inside and the outside data.

Fig.	Meas. Time/Date	Cooldown Period	Mode
1	1300 / 23-Aug-85	9 hours	FEB with SBE
2	0900 / 26-Feb-86	13 days	Pol. Protons
3	0700 / 26-Apr-86	3 hours	FEB with SBE
4	0800 / 17-Jun-86	4 days	SEB

As you can see in Figure 2 the fine structure is revealed even when the machine is cool. The dose rates vary from a few mR/h to 10,000 mR/h, where the hottest spots are;

	FEB	POL.PROT.	FEB	SEB	
	25-Aug-85	26-Feb-86	26-Apr-86	17-Jun-86	
High:	3,000	500	10,000	900	(mR/h)
	E 20	E 20	E 20	E 20	
	A 19	A 15	A 19	F 05	
	F 01	F 05	F 01	F 02	
	F 02	F 10	F 02	F 01	
	F 10	F 01	F 07	F 10	
	F 05	F 02	F 05	E 17	
	*A 15	F 07	*G 15	F 07	
	F 06	F 06	E 15	E 15	
	H 11	*A 15	*C 03	F 03	
	*G 05	E 15	F 03	F 06	
	*G 01	F 11	*I 03	H 10	
	H 10	F 03	F 10	*I 03	
	H 15	F 04	F 04	*G 08	
		H 10	F 11		
Low :	700	100	600	200	(mR/h)

Many positions are consistantly areas of high radiation. Most of these are easily accountable. For example, at E-20, F-01, and F-02 there is always high activity. This is due to the E-20 beam catcher and its downstream activity is caused by hadron cascade development. The losses in this area primarily come from transition losses. At F-05, F-10, H-05, and H-10 are the regions of extraction. A-19 is by the region of injection. Also there is found relatively high radiation in the X-15 sections throughout the ring. In these areas are the fast quadropoles used for resonance jumping during polarized proton running. These magnets have a vertical limiting aperature. There are also regions of activity which are high in one running condition but not in another. These depend on details of the running conditions which need to be better understood.

$ IV. Machine Data and Values for k.

By taking averages from the machine data saved in the morning printouts it is possible to estimate the average losses at different times in the machine cycle.

		FEB '85 RUN	FEB '86 RUN	SEB '86 RUN	
Tot. Hrs. of Run	=	330	596	400	
Av. Beam Lost	=	3.43*10**13	2.79*10**13	9.68*10**12	ppp
Av. Inj. Loss	=	1.96*10**13	1.51*10**13	5.91*10**12	ppp
Av. Cpt. Loss	=	0.90*10**13	0.74*10**13	2.76*10**12	ppp
Av. Acc. Loss	=	0.48*10**13	0.47*10**13	2.47*10**12	ppp
Av. Trn. Loss	=	0.085*10**13	0.07*10**13	0.65*10**12	ppp
Av. Ext. Loss	=	0.39*10**12	0.35*10**12	0.21*10**12	ppp
Tot. Run Bm. Lost	=	5.30*10**19	7.80*10**19	2.70*10**19	
Av. Ext. Bm. Int.	=	1.27*10**13	1.39*10**13	7.00*10**12	ppp

It is known that large beam losses occur at very specific areas in the AGS. For example, injection losses are seen at A-19 through B-5, transition losses are now primarily seen on E-20 and the beginning of F superperiod (F-1, F-2, etc.), and extraction losses occur typically on and near the extraction equipement.

Taking that the dose in these respective areas represents the loss of the beam at the respecive times in the cycle (although the real world is not this simple, it is a fairly good approximation), the following values of k were found;

	FEB '85	FEB '86	SEB '86	AVERAGE
INJECTION	4.9*10**-14	4.9*10**-14	5.6*10**-14	5.1*10**-14
TRANSITION	3.7*10**-12	5.3*10**-12	3.4*10**-12	4.1*10**-12
EXTRACTION	6.8*10**-12	4.7*10**-12	6.2*10**-12	5.9*10**-12

As you can see the values of k are relatively consistant from one run to the next. These data are plotted on graphs I-IV (see appendix for an explaination of the error bars and an example of how the values were arrived at).

Graph I is a plot of the values of k for the different times in the cycle. Although the energy dependence of k is still not precisely known it should be expected that k will be small for low energy beam and get larger with energy. Future studies will provide better detail on this dependence.

Graph II shows the values of k for the injection losses for the different runs and an average is drawn. The injection losses are assumed to be spread out through the areas A-19 and B-1 through B-5. Future studies will allow better knowlege of where and relatively how much beam is lost at injection. It is hoped that a much better value of k can then be found. It is reasurring, though, that the values of k for the different runs fall so closely together based on the simple data used in this report.

Graph III shows the values of k for the transition losses for the different runs. The transition losses were assumed to be spread out through the areas E-20 and F-1 through F-4. There are two things which are observed. First, the points are more spread out than those for injection and specifically, the two FEB runs are seperated by about one standard deviation whereas the two FEB runs for injection are exactly the same. The values for k can be expected to be more uncertain in this case since the dose on the E-20 beam catcher is not solely due to transition losses. Future studies should quantify this statement better.

Graph IV shows the values of k for the extraction losses for the different runs. The extraction losses for the FEB runs were assumed to be spread out over E-5 through E7, F-5 through F14 (SBE losses), and H-5 through H-14 (FEB losses). The extraction losses for the SEB run are assumed to be spread out over F-5 through F-14. Again, as in graph III, the values are spread out, seperated by as much as one standard deviation. This most probably is due to the larger uncertainty involved in not knowing what contributed to different losses (for example, how much of the dose by F-5 is due to cascades from E-20 at different times in the cycle). Also, a different number of points was taken from FEB to SEB running and the number of points taken was simply a guess (i.e.; where, exactly, is the extraction beam loss being lost?). Also note that the values of k for transition are very close to those for extraction. It was expected that the extraction k would be much larger than the transition k. At this time it cannot be said why they came out so closely, but that more data is needed. The best explaination, at this time, is that the E-20 dose is contributed by much more than just transition.

Table I is provided to show the kind of radionuclides that are produced in the AGS. After a long cooldown the radiation is primarily due to the long lived isotopes such as Mn, Fe, & Co.

Figures 1 - 4 show the data taken by health physics.

This method of estimating the dose rate demands that we know certain information well. Specific considerations involve better measurements of beam losses, discrimination of where the losses occur in specific areas, and better resolution of the time (energy) at which the losses occur. Then good correlations need to be made from this data to the data of the residual radiation in those specific areas.

$ V. Conclusions

It is possible to predict the peak dose rates in specific areas of the AGS based on beam losses in the machine. By considering the same relationship in greater detail and in understanding the loss patterns in the AGS (possibly from the RLRM) it should also be possible to more accurately predict the dose rate. And so a thorough understanding of the losses in the machine cycle and the amount of radiation created by these loses will provide clear insight into where to emphasize future work in getting to higher intensities at the AGS.

Acknowledgements:

We would like to thank the HP personnel for providing the data and we would like to thank B. Casey and P. Gollon for their comments and assistance.

References:

1. An Approximate Relation for the Prediction of the Dose Rate from Radioactvity Induced in High Energy Particle Accelerators.
by A. H. Sullivan, CERN
Health Physics, Vol. 23 pp.253-255; 1972

2. Induced Radioactivity. by Marcel Barbier, CERN; 1969

3. Accelerator Health Physics. by H. Wade Patterson & Ralph H. Thomas, LBL; 1973

4. Production of Radioactivity by Particle Accelerators.
by Peter J. Gollen, Fermi National Accelerator Laboratory.
IEEE Transactions on Nuclear Science, Vol. NS-23, No. 4; August '76.

Appendix: The Calculation and Uncertainty of k.

As an example of the calculation of the value of k consider the data from the 1985 FEB run. The injection dose is taken from the data taken by H.P. in the area of A-19, A-20, B-1, B-2, B-3, B-4, & B-5, which summed to 3.49 R/hr., the irradiation time was 330 hours, the cooldown time was 9 hours, and the average injected beam loss was 3.43*10**13 ppp. So from

$$k = \frac{\dot{D}}{\varphi \cdot \ln\left(\frac{T+t}{t}\right)},$$

$\dot{D}$ = 3.49 R/hr.
T = 330 hrs.
t = 9 hrs.
and φ = 3.43*10**13 ppp.
Therefore k = 4.9 * 10 ** -14.

The uncertainty in k is found using;

$$(dk)^2 = \left(\frac{\partial k}{\partial \dot{D}}\right)^2 d\dot{D}^2 + \left(\frac{\partial k}{\partial \varphi}\right)^2 d\varphi^2 + \left(\frac{\partial k}{\partial T}\right)^2 dT^2 + \left(\frac{\partial k}{\partial t}\right)^2 dt^2 .$$

By taking
$d\dot{D}$ = 10%
$d\varphi$ = 20%
dT = 10%
and dt = 10%
dk is found to be approximatly 23%. The error bars on graphs II & III are based on this value. The values for $d\dot{D}$, $d\varphi$, dT, and dt are chosen relatively arbitrarily due to no quantitative data being available. Hopefully further studies will provide better knowlege of these uncertainties as well as on improving on them.

TABLE 1

Summary of radionuclides commonly identified in materials irradiated around accelerators.

Target material	Radionuclides	Half-life
Plastics and oils	^{7}Be	53.6 days
	^{11}C	20.4 minutes
Duralumin	As above, plus	
	^{18}F	110 minutes
	^{22}Na	2.60 years
	^{24}Na	15.0 hours
Steel	As above, plus	
	^{42}K	12.47 hours
	^{43}K	22.4 hours
	^{44}Sc	3.92 hours
	^{44m}Sc	2.44 days
	^{46}Sc	84 days
	^{47}Sc	3.43 days
	^{48}Sc	1.83 days
	^{48}V	16.0 days
	^{51}Cr	27.8 days
	^{52}Mn	5.55 days
	^{52m}Mn	21.3 minutes
	^{54}Mn	300 days
	^{56}Co	77 days
	^{57}Co	270 days
	^{58}Co	72 days
	^{55}Fe	2.94 years
	^{59}Fe	45.1 days
Stainless steel	As above, plus	
	^{60}Co	5.27 years
	^{57}Ni	37 hours
	^{60}Cu	24 minutes
Copper	As above, plus	
	^{65}Ni	2.56 hours
	^{61}Cu	3.33 hours
	^{62}Cu	9.80 minutes
	^{64}Cu	12.82 hours
	^{63}Zn	38.3 minutes
	^{65}Zn	245 days

FIGURE 1

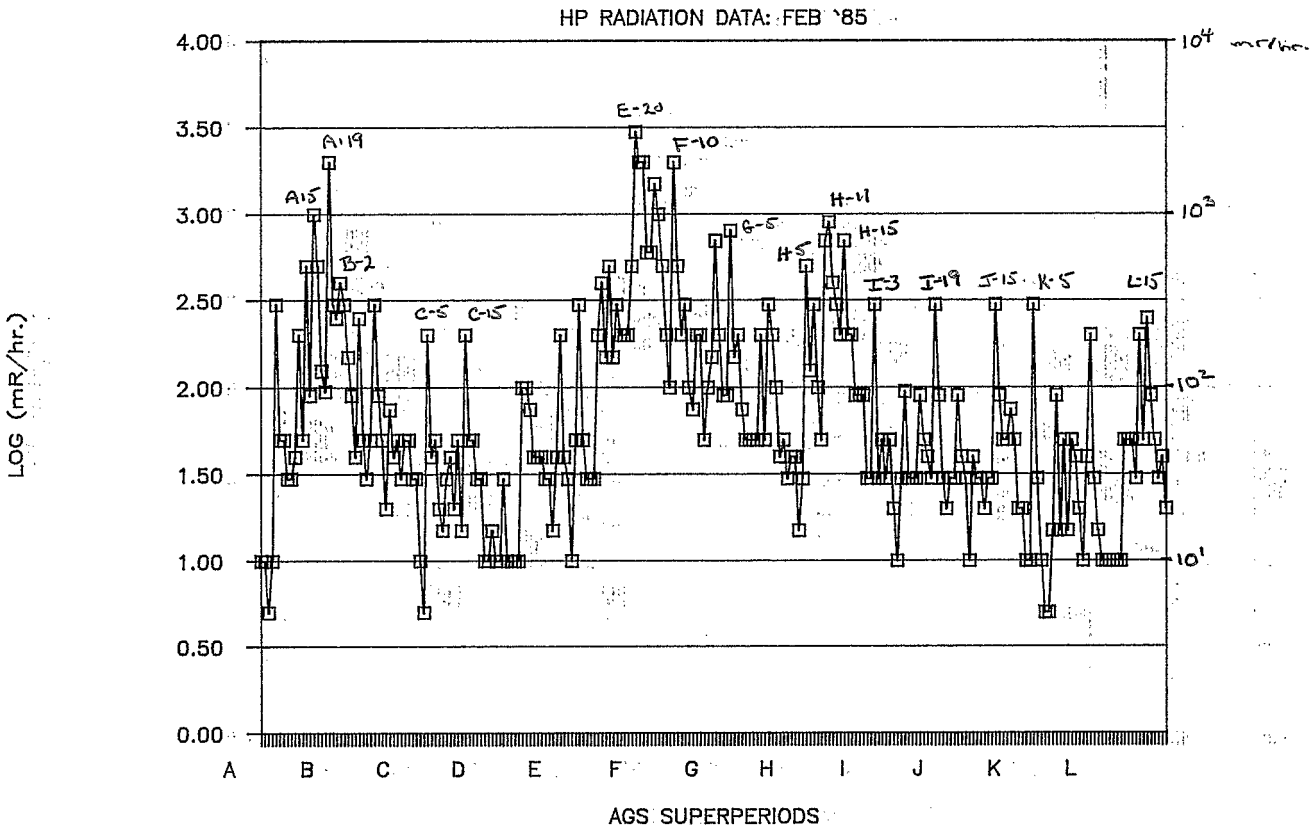

FIGURE 2

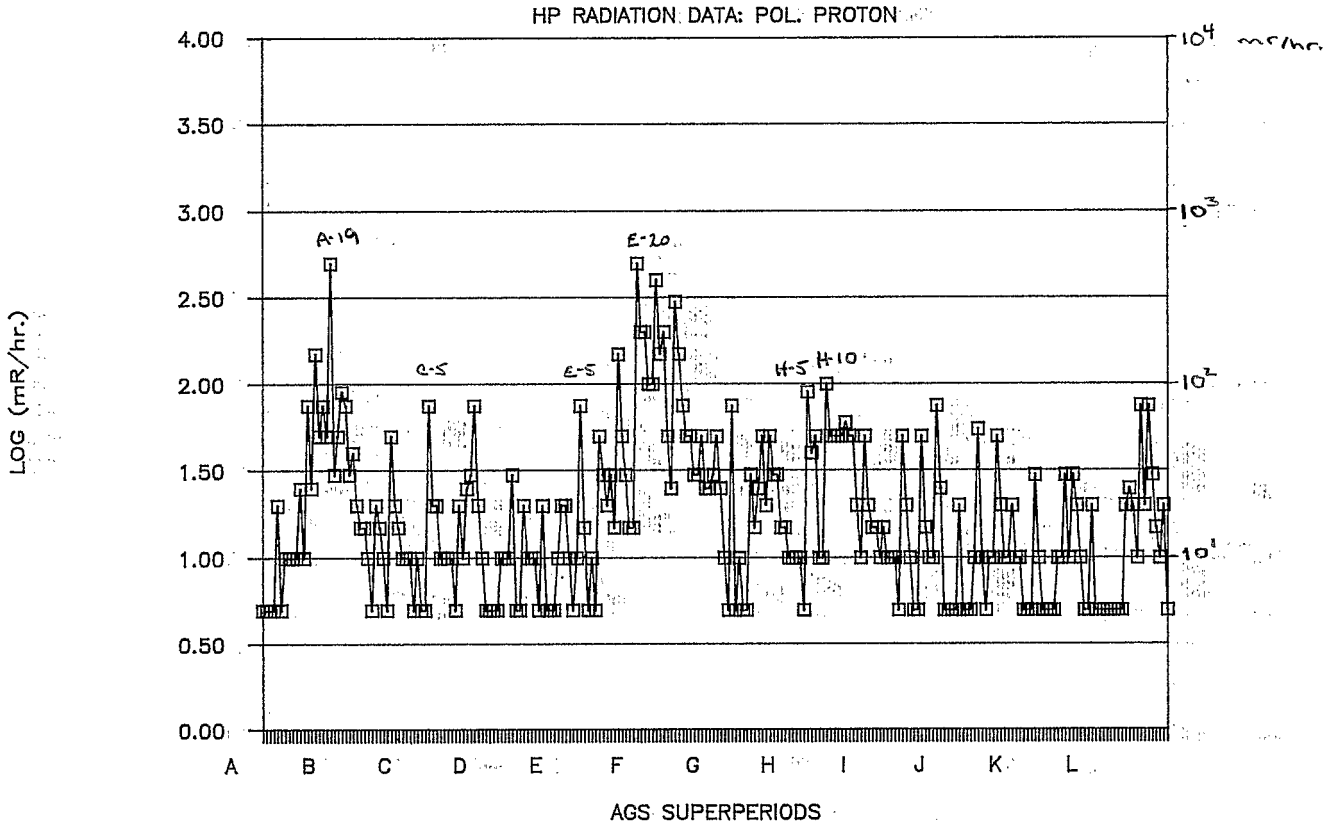

FIGURE 3

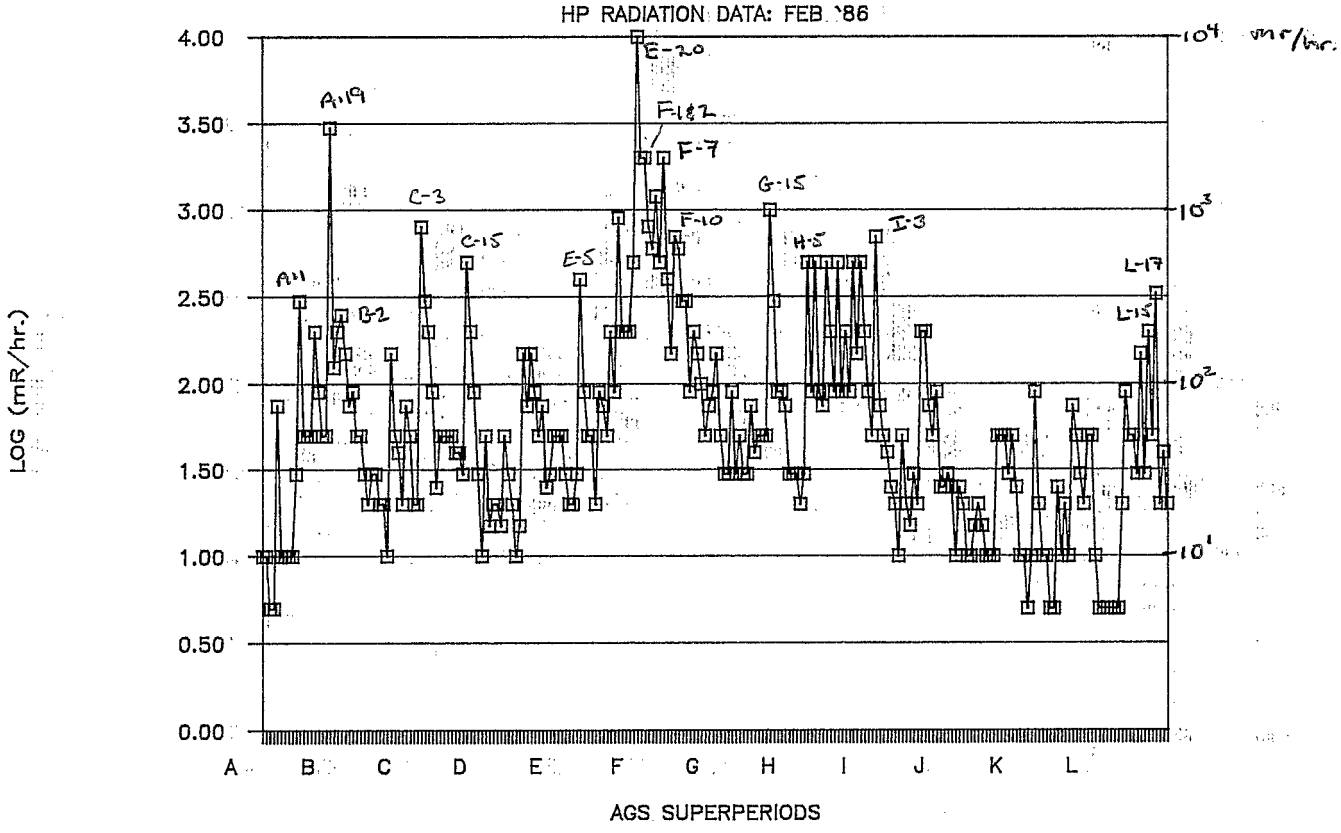

FIGURE 4

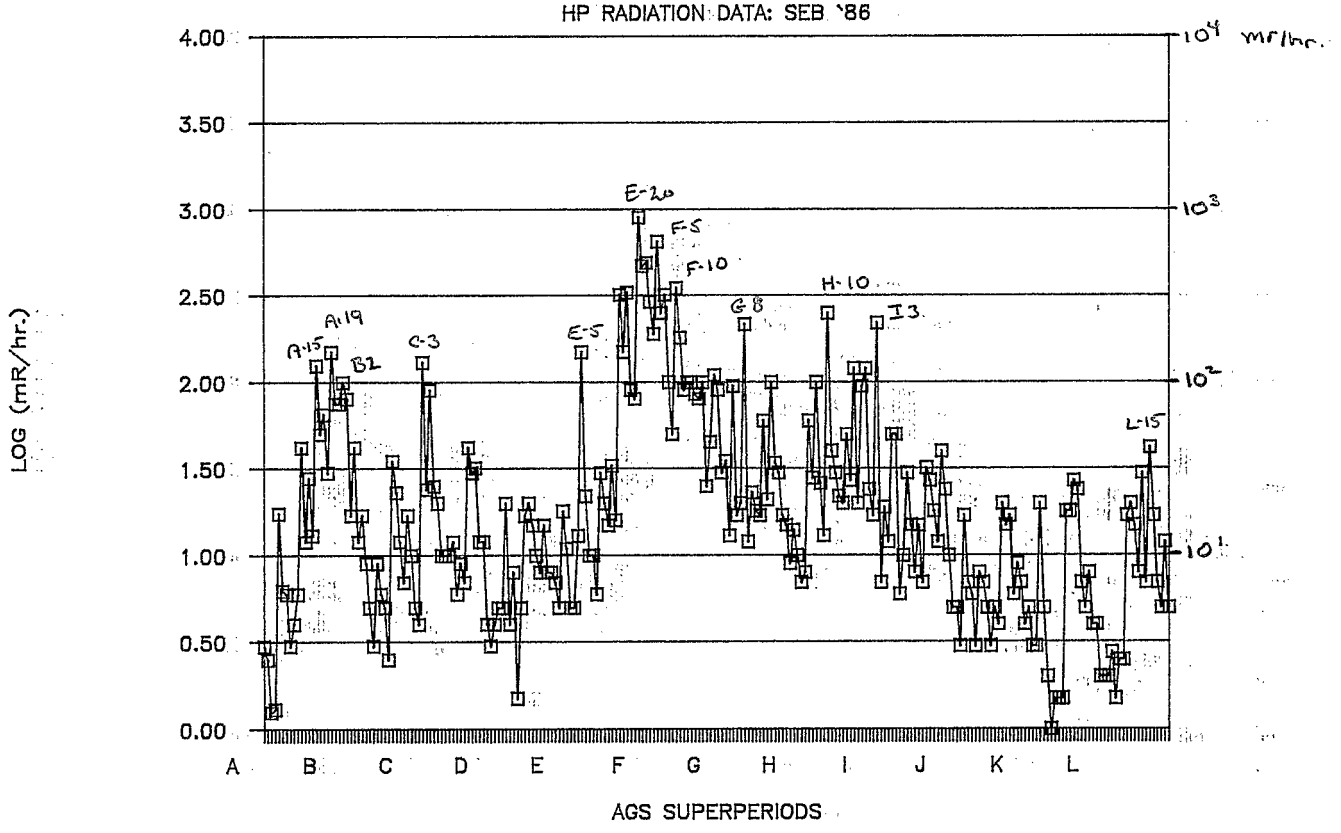

GRAPH I

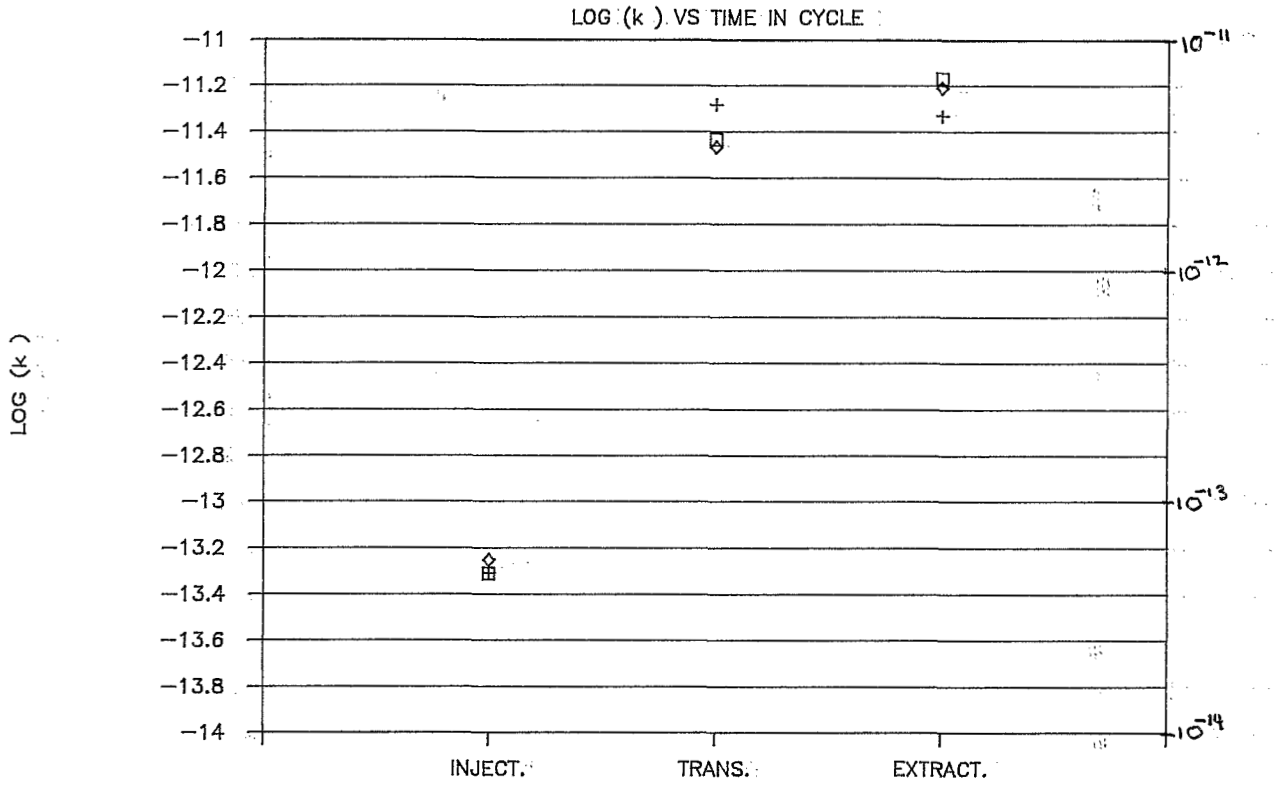

GRAPH II

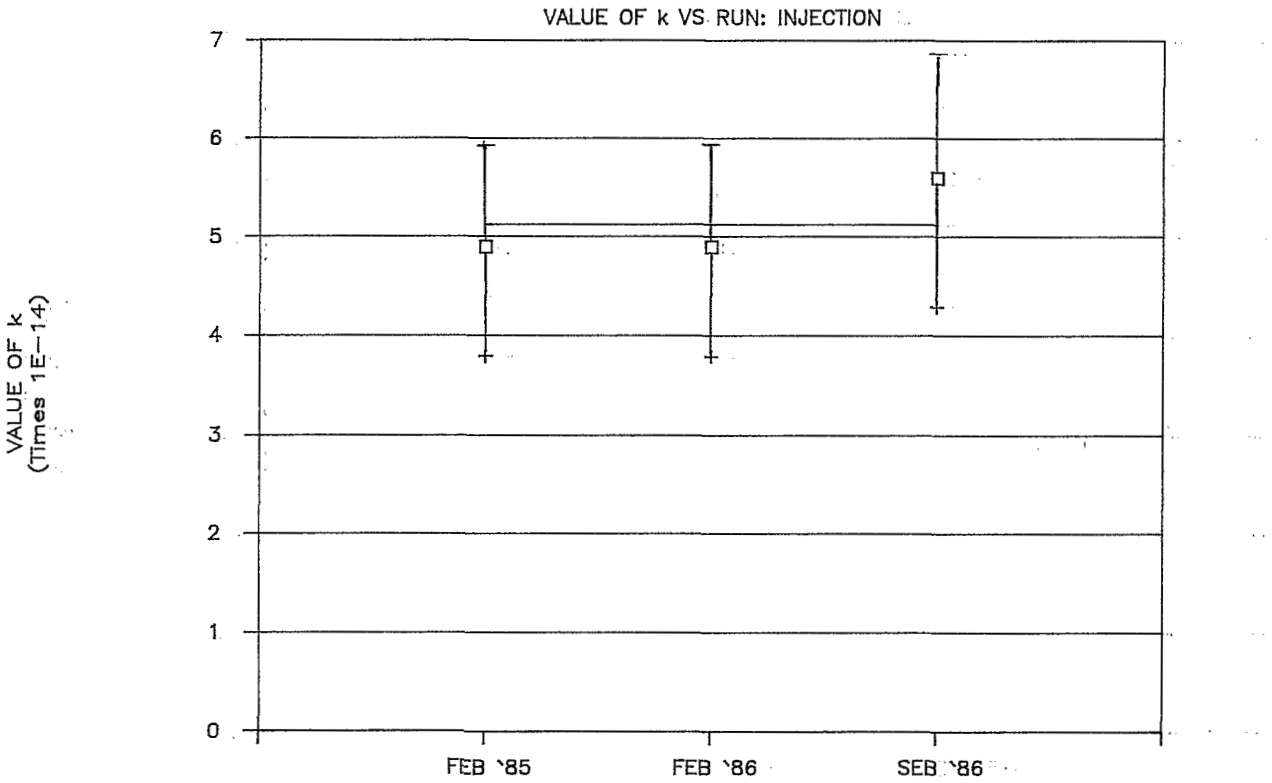

GRAPH III

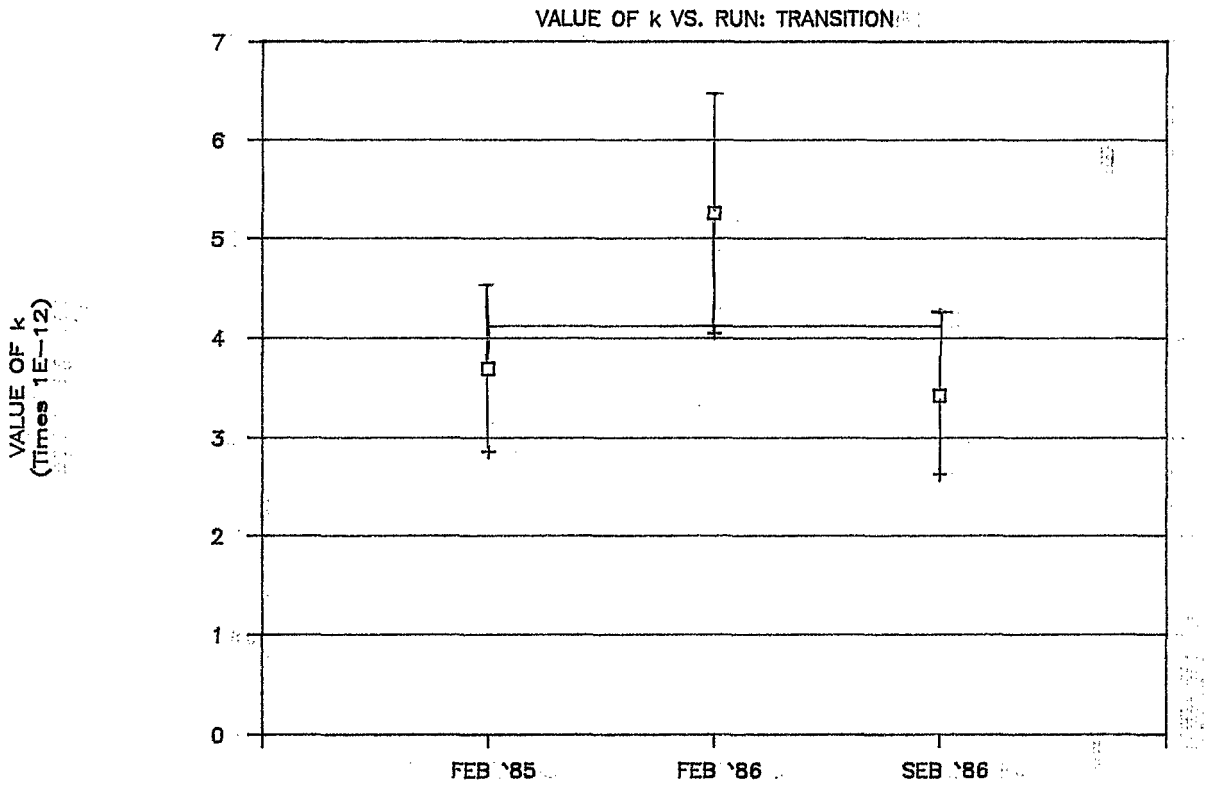

GRAPH IV